4494 *Biochemistry* **2010,** *49,* 4494–4500
DOI: 10.1021/bi902025m

BIOCHEMISTRY
including biophysical chemistry & molecular biology
Article

Enhanced Product Stability in the Hammerhead Ribozyme[†]

Irina Shepotinovskaya and Olke C. Uhlenbeck*

Department of Biochemistry, Molecular Biology, and Cell Biology, Northwestern University, Evanston, Illinois 60208

Received November 25, 2009; Revised Manuscript Received April 27, 2010

ABSTRACT: The rate of dissociation of P1, the 5′ product of hammerhead cleavage, is 100−300-fold slower in full-length hammerheads than in hammerheads that either lack or have disrupting mutations in the loop−loop tertiary interaction. The added stability requires the presence of residue 17 at the 3′ terminus of P1 but not the 2′, 3′ terminal phosphate. Since residue 17 is buried within the catalytic core of the hammerhead in the X-ray structure, we propose that the enhanced P1 stability is a result of the cooperative folding of the hammerhead around this residue. However, since P1 is fully stabilized at > 2.5 mM $MgCl_2$ while hammerhead activity continues to increase with an increase in $MgCl_2$ concentration, it is clear that the hammerhead structure in the transition state must differ from that of the product complex. The product stabilization assay is used to test our earlier proposal that different tertiary interactions modulate the cleavage rate by differentially stabilizing the core.

The folded structure of the hammerhead ribozyme can be considered to have two parts: a phylogenetically conserved catalytic core that surrounds the scissile phosphate and performs the reaction chemistry; a phylogenetically and structurally highly variable tertiary interaction that connects the ends of helix I and helix II of the secondary structure (*1*−*3*). Although the tertiary interaction is somewhat distal to the catalytic core, it indirectly influences the folding of the core by altering the geometry of the two intervening helices. The folding of the two parts is thermodynamically coupled. When the tertiary interaction is completely removed to form the less active "minimal" hammerhead, the overall orientation of the helices is not greatly altered, but the core rearranges into a quite different open conformation that is not active (*4*, *5*). Since the minimal hammerhead cleaves via the same mechanism as the full-length molecule, its low residual activity reflects a rare transient rearrangement into the active conformation of the native hammerhead (*6*). Thus, the tertiary interaction can be considered an element that stabilizes the active, but thermodynamically less stable, conformation of the core. We proposed that the variable catalytic properties observed among natural hammerheads may be in part a consequence of the degree that their different tertiary interactions stabilize the catalytically active core (*7*).

One of the catalytic core residues that undergoes a very large conformational change between the minimal and full-length hammerheads is residue 17 which is on the 5′ side of the scissile phosphate and receives the 2′, 3′ cyclic phosphate after cleavage. In the minimal hammerhead, C17 forms a single hydrogen bond with C3 and is in a quasi-helical conformation (*4*, *5*). In the full-length hammerhead, both the base and the ribose of residue 17 are buried within the catalytic core, and the backbone is aligned such that the scissile phosphate is poised for catalysis (*1*). We measure the stability of P1,[1] the 5′ product of hammerhead cleavage, by determining its dissociation rate after catalysis. Since P1 contains residue 17 on its 3′ terminus, we utilize P1 stability to evaluate the environment of residue 17 in different hammerheads under differing buffer conditions.

MATERIALS AND METHODS

P2 fragments for all of the nHHs were prepared by cotranscriptional cleavage followed by purification on denaturing gels as previously described (*8*). HH16 and other oligoribonucleotides were purchased from Integrated DNA Technologies, Inc. We prepared all 5′ product oligonucleotides containing 2′, 3′ cyclic termini using substrate oligonucleotides that extend the desired P1 by three 3′ terminal residues, incubating them with an excess of HH16, and subjecting the reaction mixture to thermocycling until they were cleaved (*8*). Single-turnover ligation assays contained 1 μM P2 and trace (2−3 nM) [5′-^{32}P]P1 in the appropriate buffer and were performed and analyzed as previously described (*7*, *8*). The P1 ligation chase protocol to measure k_3 (*9*) involved mixing 0.5 μM P2 and trace (2.5−5 nM) [5′-^{32}P]P1 in the appropriate buffer in a 90 μL reaction volume. After equilibration for 30 min at 25 °C, the chase was initiated via addition of 10 μL of 5 μM nonradioactive P1 in the same buffer, and 5 μL aliquots were removed at the desired times and terminated by addition of 10 μL of 7 M urea and 50 mM EDTA. The reaction products were separated on 20% denaturing gels, detected using a Storm PhosphorImager (Amersham Biosciences), and quantified using Image Quant (Amersham Biosciences). The dissociation rates (k_3) of 8-P1OH and 8-P1ΔC17 were determined using a similar chase strategy but were analyzed by 15% native polyacrylamide gels containing 10 mM $MgCl_2$ (*9*); 1 μM P2 was mixed with trace (2−5 nM) [5′-^{32}P]P1OH in the appropriate buffer in a 100 μL reaction volume and allowed to equilibrate at 25 °C for 30 min. To initiate the chase, 9 μL aliquots were added to 1 μL of 10 uM nonradioactive P1OH in the same buffer at appropriate times such that all the reactions could be terminated

[†]This work was supported by Grant R01GM36944 from the National Institutes of Health.

*To whom correspondence should be addressed. E-mail: o-uhlenbeck@northwestern.edu. Telephone: (847) 491-5139. Fax: (847) 491-5444.

[1]Abbreviations: EDTA, ethylenediaminetetraacetic acid; HH, hammerhead ribozyme; HEPES, *N*-(2-hydroxyethyl)piperazine-*N*′-2-ethanesulfonic acid; MES, 2-(*N*-morpholino)ethanesulfonic acid; P1, 5′ cleavage product; FRET, fluorescence resonance energy transfer.

 Published on Web 04/27/2010

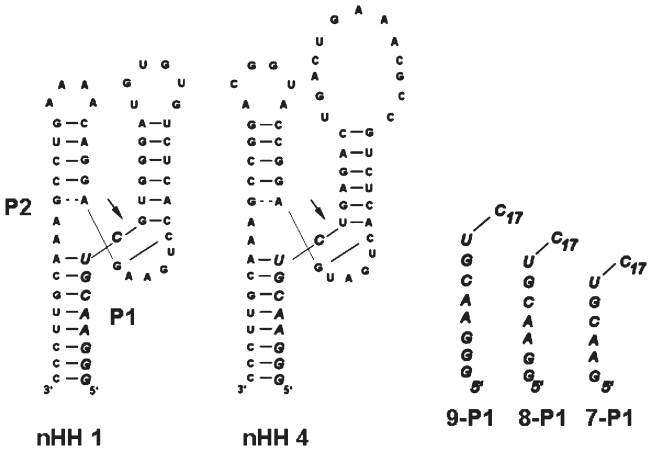

FIGURE 1: Secondary structures of two hammerhead chimeras. Arrows mark the cleavage site between the 5′ product, P1 (bold), and the 3′ product, P2. The three different P1 lengths are shown at the right.

Table 1: Kinetic Properties of nHH1 and nHH4[a]

Hammerhead				
P2	P1	k_{obs}(L) (min^{-1})	f_{eq}(L)	k_3 (min^{-1})
nHH1	7-P1	0.18 ± 0.02	0.22 ± 0.02	0.13 ± 0.04
nHH1	8-P1	0.15 ± 0.01	0.26 ± 0.01	0.0013 ± 0.0003
nHH1	9-P1	0.15 ± 0.05	0.32 ± 0.04	0.00015 ± 7 × 10^{-6}
nHH4	7-P1	0.65 ± 0.03	0.06 ± 0.004	0.17 ± 0.02
nHH4	8-P1	0.57 ± 0.16	0.12 ± 0.04	0.0022 ± 0.0005
nHH4	9-P1	0.66 ± 0.03	0.13 ± 0.01	0.0004 ± 1.4 × 10^{-5}

[a] k_{obs}(L) and f_{eq}(L) measured in 1 mM $MgCl_2$ and 50 mM MES (pH 6.0) at 25 °C and k_3 measured in 10 mM $MgCl_2$ and 50 mM HEPES (pH 7.4) at 25 °C.

simultaneously via addition of 4 μL of 50% sucrose and dyes and mixtures loaded immediately on a running native gel.

RESULTS

Stability of the Ribozyme−Product Complex. Figure 1 shows the sequences and secondary structures of the nHH1 and nHH4 chosen to initially evaluate product dissociation rates. Both these hammerheads are chimeras of natural hammerheads found in viroids and the well-studied minimal hammerhead 16. We have previously shown that both nHH1 and nHH4 can be assembled by annealing the nine-nucleotide 5′ product fragment 9-P1 with the longer 3′ product fragment P2 to form a complex that is fully active in the reverse, ligation reaction (*7*). Since it was often desirable to use shorter P1 fragments to measure product dissociation rates, it was first necessary to show that the seven- and eight-nucleotide versions of P1 that are truncated at the 5′ terminus (Figure 1) could assemble and were active. The rate of approach to equilibrium, k_{obs}, and the fraction of full-length hammerhead at equilibrium, f_{eq}(L), could be measured by mixing a low concentration of [5′-^{32}P]P1 with a saturating concentration of P2 and measuring the increased fraction of full-length molecules over time. This was most conveniently done in a 1 mM $MgCl_2$ buffer (pH 6.0) where the cleavage rate was slow enough to permit manual pipetting to be used (*7*, *10*). As shown in Table 1, both nHH1 and nHH4 have very similar values of k_{obs} and f_{eq}(L) for all three P1 lengths. The fact that 5′ truncations of P1 do not affect the catalytic properties of the hammerhead has also been found for a minimal hammerhead (*11*). This observation is not surprising since the 5′ end of P1 in helix III is well away from the folded catalytic core of the hammerhead (*1*).

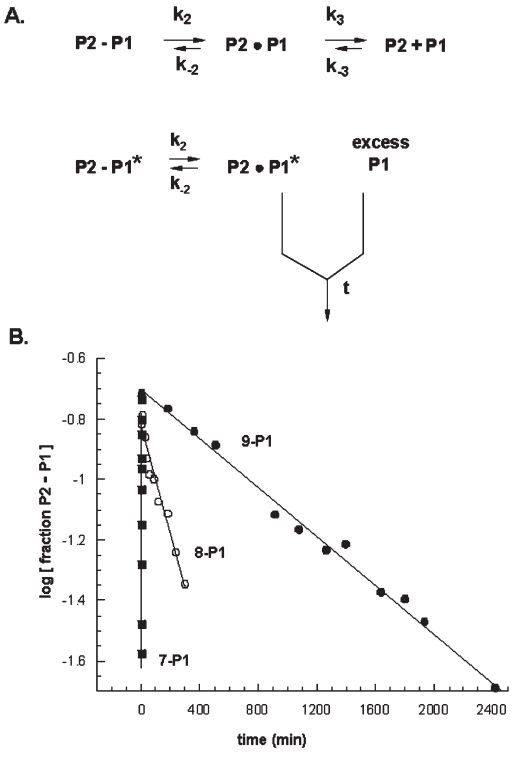

FIGURE 2: (A) Scheme for self-cleavage and product release steps (above) and design of the P1 chase protocol (below). P1* indicates 5′-^{32}P-labeled oligomer. (B) Dissociation of P1* from nHH4 in 10 mM $MgCl_2$ and 50 mM HEPES (pH 7.4) at 25 °C using the ligation chase protocol. Lines correspond to best fit first-order rates of 0.00041 min^{-1} for 9-P1 (●), 0.0028 min^{-1} for 8-P1 (○), and 0.15 min^{-1} for 7-P1 (■).

To determine k_3, the rate of dissociation of P1 from P2, a chase protocol (*9*) that relies on the very rapid cleavage−ligation equilibrium was used (Figure 2). Each [5′-^{32}P]P1 oligomer was mixed with a saturating concentration of the appropriate P2 and allowed to come to equilibrium as described above. Since the experiment was conducted at pH 7.4 instead of pH 6.0, k_{obs} is ~30-fold faster (*7*), so equilibrium is reached within seconds. At time zero, a 500-fold excess of nonradioactive P1 was added and the rate of decrease in the fraction of radiolabeled full-length hammerhead (P1−P2) was determined (Figure 2B) from aliquots quenched at varying times. Since the cleavage−ligation equilibrium is fast and the large excess of nonradioactive P1 prevents rebinding of [^{32}P]P1, the rate of P1 release was obtained (k_3). Control experiments showed that the value of k_3 for 8-P1 was not significantly affected between pH 6.0 and 8.4 (data not shown). This indicates that k_3 reflects the pH-independent helix dissociation and does not contain a contribution of the pH-dependent catalytic step. As summarized in Table 1, the values of k_3 for both nHH1 and nHH4 increased substantially as the length of P1 decreased, which is consistent with the successive removal of GC base pairs from the end of helix III.

It is striking that the value of k_3 for 9-P1 for both nHHs is 100−300-fold slower than the previously reported k_3 (0.04 min^{-1}) for the same oligonucleotide from HH16 under similar reaction conditions (*9*). While the stability of 9-P1 with respect to HH16 (ΔG° = −12.9 kcal/mol) closely approximates the value expected for an RNA duplex of the same sequence (*12*, *13*), 9-P1 binds nHH1 and nHH4 ~2.7 kcal/mol tighter than expected for an RNA

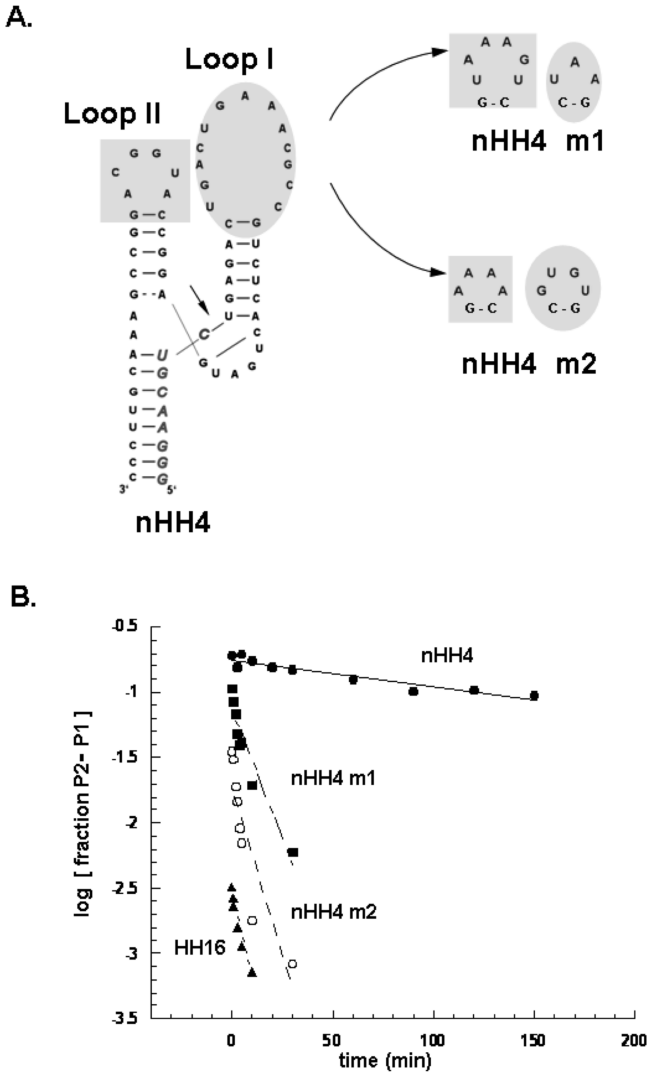

FIGURE 3: (A) Two mutations of nHH4 that change the sequences of loop 1 and loop II to disrupt the tertiary interaction. (B) Dissociation of 8-P1* from different hammerheads in 10 mM $MgCl_2$ and 50 mM HEPES (pH 7.4) at 25 °C using ligation chase experiments. First-order rates are 0.002 min^{-1} for nHH4 (●), 0.072 min^{-1} for nHH4ml (■), 0.12 min^{-1} for nHH4m2 (○), and 0.06 min^{-1} for HH16 (▲).

duplex. This is much stronger than what was observed for an additional base stacking interaction at the end of a duplex and is similar to the free energy gained from an additional, relatively stable base pair (*14*).

To confirm that the enhanced stability requires the presence of the loop−loop tertiary interaction, the rate of dissociation of 8-P1 from nHH4 was compared with the rates of dissociation of 8-P1 from nHH4ml and nHH4m2, which have mutations that disrupt the loop−loop interaction (Figure 3A). As shown in Figure 3B, the mutants gave k_3 values of 0.08 ± 0.005 min^{-1} and 0.13 ± 0.007 min^{-1} which are much faster than that of nHH4 (k_3 = 0.0022 min^{-1}) and quite similar to that of HH16 (k_3 = 0.06 min^{-1}). Control experiments measuring the ligation rate in the 1 mM $MgCl_2$ buffer (pH 6.0) gave a k_{obs} of 0.03 ± 0.005 min^{-1} for both of the mutants (data not shown) which is well below the value of 0.66 min^{-1} for nHH4. This is consistent with earlier experiments (*8*) which show that mutations that disrupt the tertiary interaction lead to lower k_{obs} values. Thus, these experiments clearly show that the enhanced stability of P1 requires an intact loop−loop tertiary interaction.

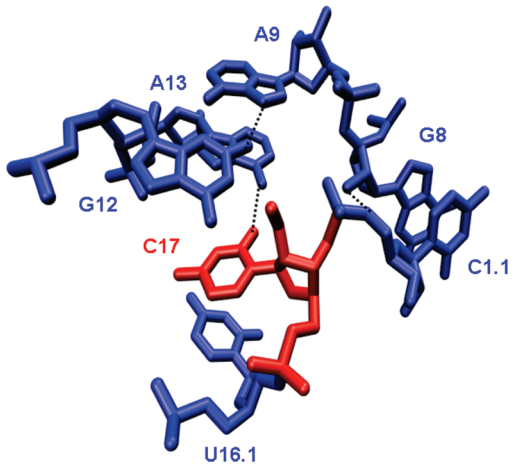

FIGURE 4: Hammerhead core structure in neighborhood of C17 (red) from Protein Data Bank entry 2GOZ. The hydrogen bonds are those suggested in ref *2*.

Role of Residue 17. In the X-ray structures of the uncleaved *Schistosoma mansoni* hammerhead (*1*) and both the uncleaved and cleaved forms of a mutant of the sTRSV hammerhead (*2*), residue 17, the 3′ terminal nucleotide of P1, forms extensive interactions with other residues in the catalytic core. In all three structures, the cytidine 17 base is packed between G12 and U16.1 and makes at least one hydrogen bond between its C2 oxygen and the amino group of A13 in the buffer used for crystallography (Figure 4). In contrast, the remaining residues of P1 make normal base pairs with P2 to form helix III. This suggests that the enhanced stability of P1 in the nHH compared to that of HH16 could be due to these interactions with C17. To test this, the rate of dissociation of 8-P1 from nHH4 was compared to those of derivatives that were missing either the 2′, 3′ cyclic phosphate (8-P1OH) or the entire residue C17 (8-P1ΔC17). Since neither of these P1 derivatives was active in ligation, a native gel had to be used to measure their dissociation rates (Figure 5A). As shown in Figure 5B, the value of k_3 for the normal 8-P1 using this native gel assay (k_3 = 0.0025) agreed well with the value previously given in Table 1 using the denaturing gel assay (k_3 = 0.0022). Interestingly, the removal of the 2′, 3′ cyclic phosphate had relatively little effect on the dissociation rate of P1 (k_3 = 0.0024 min^{-1}). This indicates that the contact between the scissile phosphate and the 2′-OH group of G8 proposed in the uncleaved hammerhead structure (*1*, *2*) is either not present or not thermodynamically important in the cleaved hammerhead. As would be expected from the structures, removal of C17 dramatically reduced the stability of 8-P1, although obtaining a dissociation rate was not straightforward since 8-P1ΔC17 was fully dissociated after reaction for 1 min (Figure 5B). To obtain a value for P1 dissociation in the absence of residue 17, chase experiments were performed using the more stable 9-P1ΔC17. As shown in Figure 5C, the rate of dissociation of this oligomer from nHH4 was virtually identical to the value for nHH4ml or HH16. Thus, removing residue 17 results in a dissociation rate that approximates the value expected for helix III. Taken together, these experiments clearly demonstrate that the enhanced binding of P1 to the hammerhead requires residue 17 as well as the loop−loop tertiary interaction.

To determine how much the identity of N17 affects k_3, the four N17 derivatives of 8-P1 were used to measure k_3, k_{obs}, and f_{eq}(L). Interestingly, the values of k_3 for the four derivatives differ by less than 3-fold (Table 2). This contrasts dramatically with very large differences in substrate binding (and presumably product binding)

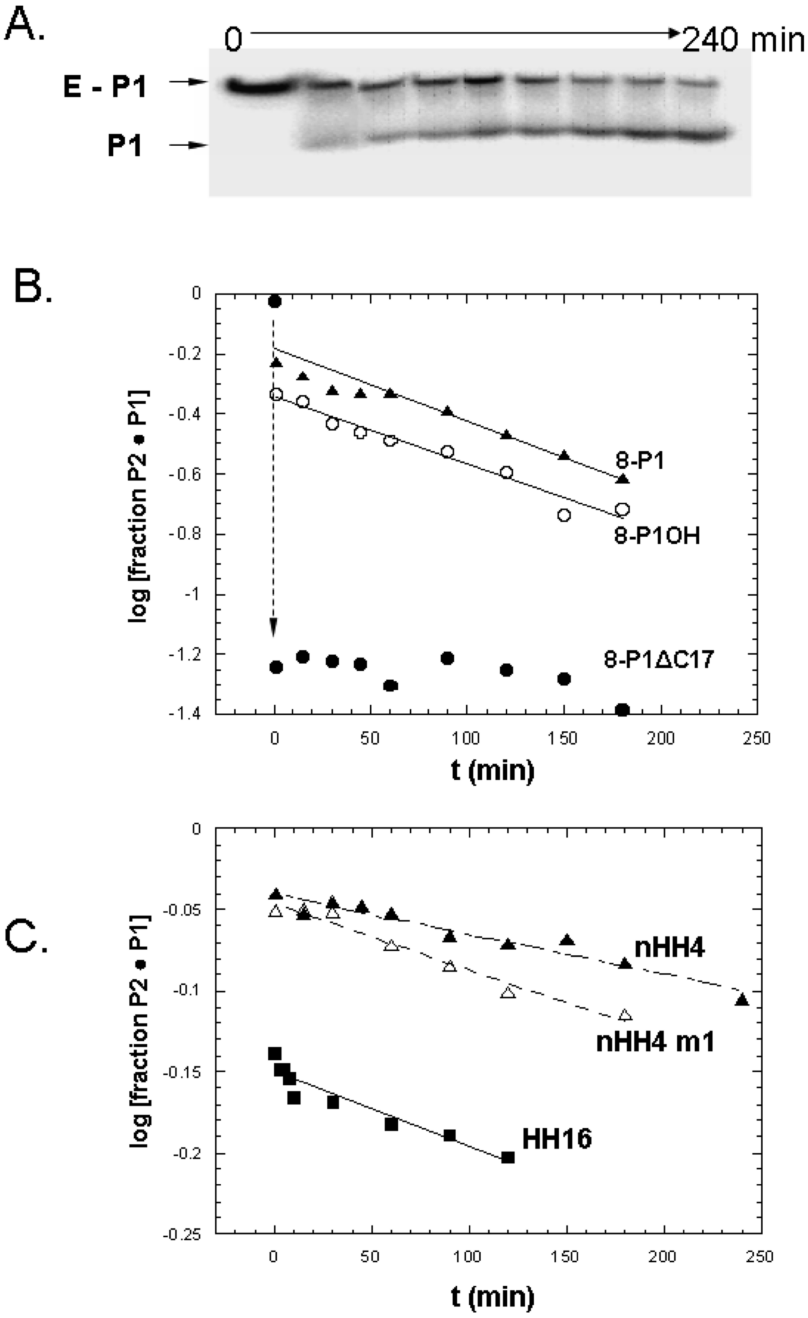

FIGURE 5: Rates of P1 release for chase experiments in 10 mM $MgCl_2$ and 50 mM HEPES (pH 7.4) at 25 °C analyzed by native gel electrophoresis. (A) Native gel showing the time course of release of 8-P1 from nHH4. (B) Dissociation rates of 0.0024 min^{-1} for 8-P1 (▲), 0.0027 min^{-1} for 8-P1OH (○), and >2 min^{-1} for 8-P1ΔC17 (●). (C) Dissociation rates for 9-P1ΔC17 are 0.51 min^{-1} for nHH4 (▲), 0.31 min^{-1} for nHH4ml (△), and 0.35 min^{-1} for HH16 (■).

Table 2: Kinetic Properties of nHH4 with Different N17 Residues[a]

N17	k_3 (min^{-1})	k_{obs}(L) (min^{-1})	f_{eq}(L)
C	0.0022 ± 0.0005	0.66 ± 0.04	0.13 ± 0.04
A	0.0048 ± 0.0001	2.33 ± 0.48	0.022 ± 0.001
U	0.0019 ± 0.0001	0.14 ± 0.01	0.06 ± 0.01
G	0.0060 ± 0.0003	0.008 ± 0.007	0.46 ± 0.04

[a]Experiments used the 8-P1 product with the indicated residue 17. k_3 measured in 10 mM $MgCl_2$ and 50 mM HEPES (pH 7.4) at 25 °C. k_{obs}(L) and f_{eq}(L) measured in 1 mM $MgCl_2$ and 50 mM MES (pH 6.0) at 25 °C.

observed for the minimal hammerhead (*15*). The G17 minimal hammerhead substrate bound the ribozyme substantially better than the other three, presumably because it made a stable Watson–Crick pair with C3. It is also important to note that while the four N17 derivatives exhibit quite similar values of k_3, their values of k_{obs} and f_{eq}(L) differ dramatically (Table 2).

Ion Dependence of k_3. Since it is well established that the concentration of $MgCl_2$ dramatically affects both the folding of the hammerhead (*16*–*18*) and the rate of catalysis (*8*, *10*, *16*, *18*–*21*), it was of interest to determine k_3 of 8-P1 at a variety of $MgCl_2$ concentrations in a pH 7.4 buffer using nHH4 and a mutant with a disrupted tertiary interaction, nHH4ml. Control experiments measuring k_{obs} at the lower $MgCl_2$ concentrations confirmed that k_{obs} remained greater than the observed value of k_3, indicating that k_3 reflected only product release and not chemistry (data not shown). As shown in Figure 6, k_3 decreases with an increase in $MgCl_2$

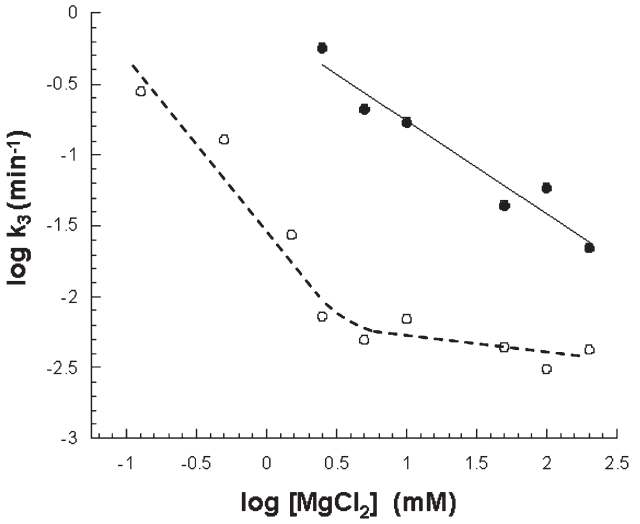

FIGURE 6: Rates of dissociation of 8-P1 from nHH4 (○) and nHH4ml (●) in 50 mM HEPES (pH 7.4) at 25 °C as a function of $MgCl_2$ concentration.

Table 3: k_3 and k_{obs} Values for nHH4 in LiCl[a]

Hammerhead			
P2	P1	k_3 (min^{-1})	k_{obs}(L) (min^{-1})
nHH4	8-P1	0.0035 ± 0.0007	1.2
nHH4ml	8-P1	0.032 ± 0.02	1.5

[a] k_{obs} (L) measured in 50 mM HEPES (pH 7.4) and 2 M LiCl at 25 °C with 9-P1, k_3 measured in 3 M LiCl, 50 mM HEPES (pH 8.4) at 25 °C with 8-P1.

concentration until a minimal value is reached at 0.007 min^{-1}. Since the slope of the plot is greater than 1, the equilibrium is cooperative as is usually seen when the magnesium concentration dependence of RNA folding is measured (*22*). However, interpretation of the data in terms of a number and affinity of magnesium ions involved in folding the core is complicated by the fact that the stability of helix III will also depend on magnesium concentration and therefore will affect k_3. The much faster k_3 values for the mutant hammerhead also decrease with an increase in magnesium concentration; however, k_3 never reaches a minimum, and the transition is much less cooperative, suggesting that folding is incomplete. Comparing the two curves in Figure 6, one can conclude that the enhanced stability of P1 is strongly magnesium-dependent with a $[MgCl_2]_{1/2}$ of ~1 mM.

Although hammerhead catalysis can occur at high concentrations of LiCl or other monovalent ions, cleavage rates are substantially slower (*23*−*26*). We recently showed that nHH4 and several other hammerheads have k_{obs} values in 2 M LiCl that were only slightly faster than that reported for HH16 in the same buffer (*7*). This suggested that the hammerhead may not fold effectively in LiCl. To test this hypothesis, the k_3 of 8-P1 was measured in 3 M LiCl and 50 mM HEPES (pH 8.5) using both nHH4 and nHH4ml. The high-pH buffer was used to ensure that the slower cleavage rate in LiCl remained faster than k_3. As reported in Table 3, the k_3 of nHH4 in this buffer is approximately 10-fold slower than for nHH4ml. While this difference is somewhat less than the 40-fold difference in k_3 observed between the two hammerheads in 10 mM $MgCl_2$ (Figure 3), the experiment clearly shows that P1 binding is strongly stabilized in the 3 M LiCl buffer. Thus, it is unlikely that the very low rate of ligation of nHH4 in LiCl (Table 3) can solely be attributed to an inefficient formation of the folded hammerhead.

Table 4: Dissociation of 7-P1 from Different Hammerheads[a]

Hammerhead	k_3 (min^{-1})	k_2 (min^{-1})	k_{-2} (min^{-1})	k_3/k_2
nHH1	0.18 ± 0.02	0.11	0.042	1.64
nHH2	0.13 ± 0.01	0.91	0.19	0.14
nHH3	0.42 ± 0.13	15	1.9	0.028
nHH4	0.20 ± 0.04	0.55	0.11	0.36
nHH5	0.67 ± 0.3	1.7	0.46	0.39
nHH6	1.1 ± 0.5	1.2	0.33	0.92
nHH8	1.3 ± 0.15	6.2	0.61	0.21

[a] k_3 measured in 10 mM $MgCl_2$ and 50 mM HEPES (pH 7.4) at 25 °C. k_2 and k_{-2} measured in 1 mM $MgCl_2$ and 50 mM MES (pH 6.0) at 25 °C from ref *7*.

Product Dissociation Rates of Different Hammerheads. Our survey of the catalytic properties of nine chimeric hammerheads derived from natural viroids and viral satellite RNAs revealed a 750-fold range in k_2 values and a 100-fold range in k_{-2} values (*7*). Since the tertiary interactions of all nine of these hammerheads were quite different, we proposed that a potential source of these catalytic differences could be the relative strengths of the tertiary interactions resulting in variable extents of hammerhead folding into a "closed", active structure. Thus, hammerheads with slower catalytic rates could have weaker tertiary interactions that result in the catalytic core folding into its active conformation less frequently. If this model were correct, one would expect to see an inverse correlation between the value of k_3 and the value of k_2 or k_{-2}. To test this, we determined the k_3 of 7-P1 with seven different hammerhead sequences. The shorter P1 was used for these experiments to yield a sufficiently rapid k_3 to conveniently measure all the hammerheads simultaneously. As shown in Table 4, the seven hammerheads exhibited k_3 values ranging from 0.13 min^{-1} for nHH2 to 1.3 min^{-1} for nHH8. Since all of these values are much slower than an estimated k_3 value of > 25 min^{-1} for the dissociation of 7-P1 from HH16 (*13*), the catalytic cores of all the natural hammerheads significantly stabilize P1. However, the range of values of k_3 is much less than the range observed for k_2 or k_{-2}, so the k_2/k_3 ratio varies considerably. While these data support the idea that different tertiary interactions lead to differential stabilization of P1, they are unlikely to solely determine the cleavage properties of different hammerheads.

DISCUSSION

A simple chase protocol was used to show that P1, the 5′ product of hammerhead cleavage, dissociates 100−300-fold more slowly from the intact hammerhead than from mutants that disrupt the tertiary interactions required for efficient folding of the core and rapid cleavage. A slow rate of dissociation of P1 from the *S. mansoni* hammerhead has been reported (*20*), but not systematically compared with that of a hammerhead lacking the stabilizing tertiary interaction. The X-ray structures of both cleaved and uncleaved hammerhead (*1*, *2*) suggest that the approximately 2.7 kcal/mol extra binding energy of P1 is the result of the catalytic core folding around the 3′ terminal C17 residue. This was supported by finding that removal of C17 from P1 weakens binding to the level found for hammerheads that disrupt or are missing the tertiary interactions. We therefore propose that the added stability of P1 indirectly measures the folding of the core of the cleaved hammerhead. Thus, the product

dissociation rate provides a simple assay to evaluate the folding of the catalytic core when perturbations in the reaction conditions or the hammerhead sequence are introduced.

FRET (*17*, *18*, *27*) and EPR (*16*) assays have been developed that also measure hammerhead folding by placing probes that monitor the close approach of helices I and II that occurs upon formation of the stabilizing tertiary interaction. By measuring a thermodynamic effect associated with folding of a different part of the hammerhead, the product dissociation assay can be considered to complement the spectroscopic assays. It is interesting that the two types of assays give very similar results when hammerhead folding was monitored as a function of magnesium ion concentration. Spin labeling and FRET experiments using the uncleaved *S. mansoni* hammerhead found that tertiary folding was complete between 2 and 4 mM $MgCl_2$ (*16*−*18*). Here we show that dissociation of P1 from nHH4 reaches a maximum by 2−3 mM $MgCl_2$. Thus, despite the very different sequences of the hammerheads, their cleavage states, and the fact that the folding assays monitor different parts of the hammerhead structure, the magnesium dependence is very similar. This presumably reflects the fact that the entire hammerhead folds as a single cooperative unit as the magnesium ion concentration is increased. Indeed, many smaller RNAs with tertiary structures fold cooperatively over a similar range of magnesium ion concentrations (*22*).

Interestingly, although the overall folding of the hammerhead is complete by 2−3 mM $MgCl_2$, hammerhead cleavage or ligation rates continue to increase with an increase in $MgCl_2$ concentration and saturation is not always observed even at concentrations in excess of 100 mM $MgCl_2$ (*8*, *10*, *16*, *20*). This implies that there is a very weakly binding magnesium ion that participates in catalysis but is only present at low occupancy with 10 mM $MgCl_2$ (*16*, *18*). Although it is tempting to speculate that this weakly binding ion is located in the neighborhood of the catalytic site and participates in the reaction chemistry (*21*, *28*), experiments establishing this have not yet been conducted. An alternative possibility is that the higher magnesium ion concentration leads to a different structure of the hammerhead not detected by the spectroscopic or product dissociation assays that more closely resemble the transition state. Such a structural change could be substantial or could simply involve a small rearrangement in the hydrogen bonding network but does not affect the stability of P1. Since the available crystal structures were determined at lower magnesium concentrations, they are unlikely to reflect this more active form.

High concentrations of LiCl were also able to greatly stabilize product binding when a stable tertiary interaction was present. Thus, in agreement with the spectroscopic experiments (*17*, *18*), the hammerhead is substantially folded at high monovalent ion concentrations. This means that the nearly 1000-fold slower hammerhead cleavage rate observed in the LiCl buffer is not simply due to the hammerhead remaining in its open, inactive conformation. It is possible that although the core folds, it does not fold correctly in 3 M LiCl, perhaps because the monovalent lithium ion cannot effectively coordinate phosphate 9 or 1.1 in the folded structure (*2*, *24*). Alternatively, it remains possible that efficient hammerhead catalysis requires the participation of a divalent ion as either a Lewis acid or base, a function the lithium ion cannot effectively provide.

While the presence of residue 17 was critical for the enhanced binding of the P1 product, the P1 dissociation rates of the different N17 derivatives were nearly identical. This was somewhat unexpected since the different N17 residues exhibit quite different stacking propensities. However, since the other N17 derivatives would be expected to fit into the catalytic core in different (currently unknown) ways, interpretation of this thermodynamic equivalence is not possible. Although the very different catalytic rates of the N17 hammerheads (*6*) suggest that they all must have different transition state structures, it is currently difficult to relate these to the P1 dissociation data. A systematic comparison of substrate binding, product binding, and catalytic rates of a series of N17 derivatives will be needed to understand this issue (*29*).

Our earlier proposal that the catalytic diversity observed among natural hammerheads is solely due to the differential ability of the tertiary domains to stabilize the core (*7*) is unlikely to be correct. Although the relatively small variation of the values of k_3 among different hammerheads may indicate that some of the natural hammerheads fold less well than others, the fact that their cleavage rates vary by much more than k_3 indicates that other structural differences among the nHHs must significantly influence k_{obs}. A strong candidate is the "bulged" nucleotide between A9 and G10.1 present in the faster cleaving nHH3, nHH5, and nHH8. It is well established that the presence of this element in the minimal hammerhead increases the cleavage rate and alters the structure or dynamics of the molecule (*30*, *31*). Perhaps because of its proximity to a metal ion binding site, the bulge also appears to alter the magnesium dependence of cleavage (*7*). Thus, it seems possible that catalytic cores containing the bulge could have intrinsically different folding and cleavage properties and result in different k_2 and k_3 values. Systematic mutagenesis will be required to dissect out the relative effects of tertiary interactions and core sequences of hammerhead folding and catalysis.

It is interesting to compare the hammerhead with the hairpin, another type of self-cleavage motif used by satellite viruses for genome replication (*32*, *33*). Although the structure of the hairpin is very different from the structure of the hammerhead, it can also be considered as having a core that performs the reaction chemistry and a peripheral motif (a four-helix junction) that stabilizes the core (*29*, *34*−*36*). In several respects, these two parts of the hairpin perform functions analogous to those of the hammerhead. The presence of the four-helix junction stabilizes the binding of the 3′ product of the hairpin by ~50-fold (*37*), an effect similar in magnitude to the 100−300-fold stabilization of the 5′ product of the hammerhead by the loop−loop interaction seen here. As a result, although the hairpin is intrinsically much better at ligation than the hammerhead, in both cases the presence of the peripheral domain significantly increases K_{int}, the ratio of ligated to cleaved forms at equilibrium. Thus, the peripheral domain causes K_{int} for the hairpin to increase from 6 to 30 (*37*), while the peripheral domains of hammerheads increase K_{int} from 0.01 to as high as 0.5 (*7*). Although the peripheral domains of the hairpin and the hammerhead have similar roles in setting K_{int}, they function quite differently in reaching the transition state. In the case of the hairpin, the value of k_{obs} is only slightly greater (18 min^{-1} vs 2.9 min^{-1}) in the presence of the four-helix junction. In contrast, k_{obs} for the hammerhead is increased by more than 800-fold (from 1 to 890 min^{-1}) when the tertiary interaction is present. Thus, the catalytic core of the hairpin is quite stable on its own, while the core of the hammerhead depends critically on the tertiary interaction to form. It is possible that these energetic differences in the architecture of the two self-cleaving domains underlie the predominance of the hairpin in the minus strand of satellite viruses.

REFERENCES

1. Martick, M., and Scott, W. G. (2006) Tertiary contacts distant from the active site prime a ribozyme for catalysis. *Cell 126*, 309–320.
2. Chi, Y. I., Martick, M., Lares, M., Kim, R., Scott, W. G., and Kim, S. H. (2008) Capturing hammerhead ribozyme structures in action by modulating general base catalysis. *PLoS Biol. 6*, 2060–2068.
3. Fedor, M. J. (2009) Comparative enzymology and structural biology of RNA self-cleavage. *Annu. Rev. Biophys. 38*, 271–299.
4. Scott, W. G., Murray, J. B., Arnold, J. R., Stoddard, B. L., and Klug, A. (1996) Capturing the structure of a catalytic RNA intermediate: The hammerhead ribozyme. *Science 274*, 2065–2069.
5. Pley, H. W., Flaherty, K. M., and McKay, D. B. (1994) Three-dimensional structure of a hammerhead ribozyme. *Nature 372*, 68–74.
6. Nelson, J. A., and Uhlenbeck, O. C. (2008) Minimal and extended hammerheads utilize a similar dynamic reaction mechanism for catalysis. *RNA 14*, 43–54.
7. Shepotinovskaya, I. V., and Uhlenbeck, O. C. (2008) Catalytic diversity of extended hammerhead ribozymes. *Biochemistry 47*, 7034–7042.
8. Nelson, J. A., Shepotinovskaya, I., and Uhlenbeck, O. C. (2005) Hammerheads derived from sTRSV show enhanced cleavage and ligation rate constants. *Biochemistry 44*, 14577–14585.
9. Hertel, K. J., Herschlag, D., and Uhlenbeck, O. C. (1994) A kinetic and thermodynamic framework for the hammerhead ribozyme reaction. *Biochemistry 33*, 3374–3385.
10. Canny, M. D., Jucker, F. M., Kellogg, E., Khvorova, A., Jayasena, S. D., and Pardi, A. (2004) Fast cleavage kinetics of a natural hammerhead ribozyme. *J. Am. Chem. Soc. 126*, 10848–10849.
11. Hertel, K. J., Herschlag, D., and Uhlenbeck, O. C. (1996) Specificity of hammerhead ribozyme cleavage. *EMBO J. 15*, 3751–3757.
12. Hertel, K. J., Stage-Zimmermann, T. K., Ammons, G., and Uhlenbeck, O. C. (1998) Thermodynamic dissection of the substrate-ribozyme interaction in the hammerhead ribozyme. *Biochemistry 37*, 16983–16988.
13. Turner, D. H., Sugimoto, N., and Freier, S. M. (1988) RNA structure prediction. *Annu. Rev. Biophys. Chem. 17*, 167–192.
14. Turner, D. H., and Mathews, D. H. (2010) NNDB: The nearest neighbor parameter database for predicting stability of nucleic acid secondary structure. *Nucleic Acids Res. 38*, D280–D282.
15. Baidya, N., Ammons, G. E., Matulic-Adamic, J., Karpeisky, A. M., Beigelman, L., and Uhlenbeck, O. C. (1997) Functional groups on the cleavage site pyrimidine nucleotide are required for stabilization of the hammerhead transition state. *RNA 3*, 1135–1142.
16. Kim, N. K., Murali, A., and DeRose, V. J. (2005) Separate metal requirements for loop interactions and catalysis in the extended hammerhead ribozyme. *J. Am. Chem. Soc. 127*, 14134–14135.
17. Penedo, J. C., Wilson, T. J., Jayasena, S. D., Khvorova, A., and Lilley, D. M. (2004) Folding of the natural hammerhead ribozyme is enhanced by interaction of auxiliary elements. *RNA 10*, 880–888.
18. Boots, J. L., Canny, M. D., Azimi, E., and Pardi, A. (2008) Metal ion specificities for folding and cleavage activity in the Schistosoma hammerhead ribozyme. *RNA 14*, 2212–2222.
19. Roychowdhury-Saha, M., and Burke, D. H. (2006) Extraordinary rates of transition metal ion-mediated ribozyme catalysis. *RNA 12*, 1846–1852.
20. Canny, M. D., Jucker, F. M., and Pardi, A. (2007) Efficient ligation of the Schistosoma hammerhead ribozyme. *Biochemistry 46*, 3826–3834.
21. Osborne, E. M., Schaak, J. E., and Derose, V. J. (2005) Characterization of a native hammerhead ribozyme derived from schistosomes. *RNA 11*, 187–196.
22. Grilley, D., Soto, A. M., and Draper, D. E. (2006) Mg^{2+}-RNA interaction free energies and their relationship to the folding of RNA tertiary structures. *Proc. Natl. Acad. Sci. U.S.A. 103*, 14003–14008.
23. Takagi, Y., Inoue, A., and Taira, K. (2004) Analysis on a cooperative pathway involving multiple cations in hammerhead reactions. *J. Am. Chem. Soc. 126*, 12856–12864.
24. O'Rear, J. L., Wang, S., Feig, A. L., Beigelman, L., Uhlenbeck, O. C., and Herschlag, D. (2001) Comparison of the hammerhead cleavage reactions stimulated by monovalent and divalent cations. *RNA 7*, 537–545.
25. Curtis, E. A., and Bartel, D. P. (2001) The hammerhead cleavage reaction in monovalent cations. *RNA 7*, 546–552.
26. Murray, J. B., Seyhan, A. A., Walter, N. G., Burke, J. M., and Scott, W. G. (1998) The hammerhead, hairpin and VS ribozymes are catalytically proficient in monovalent cations alone. *Chem. Biol. 5*, 587–595.
27. Bassi, G. S., Mollegaard, N. E., Murchie, A. I., and Lilley, D. M. (1999) RNA folding and misfolding of the hammerhead ribozyme. *Biochemistry 38*, 3345–3354.
28. Lee, T. S., Giambasu, G. M., Sosa, C. P., Martick, M., Scott, W. G., and York, D. M. (2009) Threshold occupancy and specific cation binding modes in the hammerhead ribozyme active site are required for active conformation. *J. Mol. Biol. 388*, 195–206.
29. Cottrell, J. W., Kuzmin, Y. I., and Fedor, M. J. (2007) Functional analysis of hairpin ribozyme active site architecture. *J. Biol. Chem. 282*, 13498–13507.
30. Warashina, M., Kuwabara, T., Nakamatsu, Y., Takagi, Y., Kato, Y., and Taira, K. (2004) Analysis of the conserved P9-G10.1 metal-binding motif in hammerhead ribozymes with an extra nucleotide inserted between A9 and G10.1 residues. *J. Am. Chem. Soc. 126*, 12291–12297.
31. De la Pena, M., and Flores, R. (2001) An extra nucleotide in the consensus catalytic core of a viroid hammerhead ribozyme: Implications for the design of more efficient ribozymes. *J. Biol. Chem. 276*, 34586–34593.
32. Fedor, M. J. (2000) Structure and function of the hairpin ribozyme. *J. Mol. Biol. 297*, 269–291.
33. Buzayan, J. M., Gerlach, W. L., Bruening, G., Keese, P., and Gould, A. R. (1986) Nucleotide sequence of satellite tobacco ringspot virus RNA and its relationship to multimeric forms. *Virology 151*, 186–199.
34. Thomson, J. B., and Lilley, D. M. (1999) The influence of junction conformation on RNA cleavage by the hairpin ribozyme in its natural junction form. *RNA 5*, 180–187.
35. Walter, N. G., Hampel, K. J., Brown, K. M., and Burke, J. M. (1998) Tertiary structure formation in the hairpin ribozyme monitored by fluorescence resonance energy transfer. *EMBO J. 17*, 2378–2391.
36. Wilson, T. J., Nahas, M., Ha, T., and Lilley, D. M. (2005) Folding and catalysis of the hairpin ribozyme. *Biochem. Soc. Trans. 33*, 461–465.
37. Fedor, M. J. (1999) Tertiary structure stabilization promotes hairpin ribozyme ligation. *Biochemistry 38*, 11040–11050.